Journal of
Polymer & Composites
https://journals.stmjournals.com/jopc
ISSN: 2321-2810 (Online)
ISSN: 2321-8525 (Print)
Volume 14, Special Issue 2, 2026
DOI (Journal): 10.37591/JoPC
Research JoPC

Thermal and Mechanical Properties of Zn-Fap Composites

Hazari Naresh[1], Nagasri Sunkara Saihari[2], M.S. Srinivasa Rao[3], Aedula Manoj Kumar[4], Kyadagiri Shashank[5], T.S. Krishna Kumar[6,*]

Abstract

The aerospace and automotive industries have experienced a substantial surge in interest in innovative composite systems driven by the ongoing demand for lightweight, high-performance materials. In this study, the mechanical properties of zinc (Zn) matrix composites reinforced with fluorapatite particles (Fap) are examined as a function of thermal treatment. Within the context of this investigation, we endeavoured to create composite materials containing Zinc-Fluorapatite powder. Stir casting was used to produce both Pure zinc composites and Fap composites. A variety of compositions were taken, and all samples underwent mechanical characterization, namely, a tensile test. The samples were heat-treated in the furnace after casting to assess their behaviour. The findings suggest that mechanical properties are highly dependent on the heat treatment used. The ultimate tensile strength of the samples treated at a specific temperature for a specific duration was found to be significantly increased. This was because particle dispersion improved, and interfacial bonding between the Zn matrix and the Fap reinforcement increased. The yield strength of the 1% Fap composites was found to be 40 MPa, while their ultimate tensile strength was found to be 60 MPa. The yield strength of the pure zinc sample is 55MPa, while the ultimate tensile strength of the sample is 70MPa.

Keywords: Zinc- fluorapatite composites, thermal analysis, mechanical properties, thermal treatment

INTRODUCTION

Heat treatment significantly influences the microstructure and mechanical properties of Zn-Fap (Zinc-Fluorapatite) composite materials [1]. The process can alter the crystal structure, grain size, phase formation, and defect density, thereby modifying mechanical properties like hardness, toughness, and elastic modulus [2]. In Zn-Fap composites, heat treatment can enhance sinterability, promoting densification and improving mechanical performance; it may also affect bioactivity by altering surface morphology or porosity [3, 4]. Heat treatment can induce several microstructural changes in Zn-based composites [5–7]. In Al-Zn-Mg-Cu alloys, heat treatment refines the grain structure, which directly affects mechanical strength [8]. Similarly, in Zn-Al alloys and Zn-Al/ZrB2 composites, heat treatment at 250 °C for 3 hours refines the grain structure and improves hardness. Nevertheless, elevated temperatures may reduce hardness and increase particle size. The alloy composition and the heat treatment parameters, including temperature and duration, determine the specific alterations.[9]. The high-temperature treatment of CVI-Cansas-III/PyC/SiC composites showed degradation of Cansas-III

*Author for Correspondence
T.S. Krishna Kumar

[1,2]Assistant Professor, Department of Mechanical Engineering, VNR Vignana Jyothi Institute of Engineering and Technology, Hyderabad, Telangana, India
[3]Senior Assistant Professor, Department of Mechanical Engineering, VNR Vignana Jyothi Institute of Engineering and Technology, Hyderabad, Telangana, India
[4,5]Student, Department of Mechanical Engineering, VNR Vignana Jyothi Institute of Engineering and Technology, Hyderabad, Telangana, India
[6]Assistant Professor, Department of Automobile Engineering, VNR Vignana Jyothi Institute of Engineering and Technology, Hyderabad, Telangana, India

Received Date: October 01, 2025
Accepted Date: February 11, 2026
Published Date: April 20, 2026

Citation: Hazari Naresh, Nagasri Sunkara Saihari, M.S. Srinivasa Rao, Aedula Manoj Kumar, Kyadagiri Shashank, T.S. Krishna Kumar. Thermal and Mechanical Properties of Zn-Fap Composites. Journal of Polymer & Composites. 2026; 14(Special Issue 2): S1101–S1110p.

fibers with increasing temperature, resulting in a reduction of fiber properties due to pyrolysis of the SiOC phase inside the fibers. The mechanical properties of Zn-FAP composites, such as tensile strength, hardness, and wear resistance, are significantly affected by heat treatment [10–12]. In SiC/6061 composites, heat treatment increases both yield strength and ultimate tensile strength due to the precipitation of β' phase [13]. Similarly, annealing heat treatment on Al–Zn–Mg/3 wt.% Al2O3 composites improves the distribution of alumina reinforcement particles, thereby enhancing mechanical properties [14]. The effect of heat treatment on Al-Zn-Mg-Cu alloys shows significant improvements in hardening and plastic properties [15]. The study of Ti-TiAl laminate composites demonstrated that heat treatment enhances fracture toughness and elongation by reducing dislocations and substructures in the Ti-43Al-9V alloy [16]. In this study, Zn-20 wt% Mg composites were fabricated via a low-temperature electric-field-assisted sintering technique using high-purity Mg and Zn powders. The composites achieved a relative density of 99.5%, with microstructural characterization revealing a dual-phase structure of Zn and Mg, featuring intimate particle-to-particle connections. XRM-CT slice analysis revealed that corrosion cracks preferentially initiated at sites of Mg particle aggregation, where Mg experienced more severe corrosion [17]. This study examines adding magnesium (Mg) and neodymium (Nd) as alloying elements and using hot extrusion to produce Zn-based alloys with improved mechanical and biological properties, suitable for moderately weight-bearing orthopedic applications. The Zn-0.1Mg-1Nd alloy produced has small grains with an average size of 1.36 µm. This makes it stronger than pure Zn (71 MPa) and increases its tensile strength to 381 MPa. It also stretches much more, from 10.7% to 17.7% [18]. Compositing metal-metal composites with conventional zinc-aluminium alloy ZA-27 as a matrix and titanium microparticles (about 10 µm) as a secondary phase was explored. 1-2 wt% Ti microparticles. Small amounts (0.5 wt%) of 20–30 nm alumina nanoparticles are utilized as reinforcement. The submitted research examined the feasibility of making such composites and the effects of Ti and alumina nanoparticles on their microstructure, mechanical, and tribological properties. Microstructure, worn Surfaces, and mechanical properties were analyzed using a scanning electron microscope, and Vickers microhardness values [19]. Zinc matrix composites with graphene exhibit tensile strengths up to 254 MPa at 0.7 wt% graphene reinforcement, 126% higher than pure zinc, while maintaining elongation near 17%. Fap replacement in ceramics boosts fracture strength, hardness, and elastic modulus with higher sintering temperatures and Fap content [20]. The selection of fluorapatite as a ceramic reinforcement is driven by its inherent advantages in chemical stability, acid resistance, biocompatibility, and the ability to significantly improve the mechanical properties of various composites. Its versatility in synthesis and application positions it as a preferred material for advanced biomedical engineering [21].

In this research work, a zinc-fluorapatite composite material was prepared by the stir-casting method, and its Microstructural properties and Mechanical characterization were studied.

MATERIALS AND METHODOLOGY

Fabrication Procedure for Zinc-Fluorapatite Composites

The zinc metal ingots are placed in a crucible furnace as shown in Figure 1, which is then heated to approximately 420°C, The melting point of zinc is shown in Figure 2. Fluorapatite powder with a particle size of 100µm is preheated up to 175 °C to create wettability. Once the zinc reaches a liquid state, fluorapatite powder (Fap) is slowly introduced into the molten zinc which is shown in Figure 3. This addition is done gradually to ensure controlled dispersion of the powder, preventing agglomeration of particles. After adding the Fap powder, the molten zinc and Fap mixture is continuously stirred at a speed of 350 rpm for 15 minutes. This stirring ensures a uniform distribution of Fap particles throughout the zinc melt, preventing uneven particle clustering that could affect the composite’s properties.

ISSN: 2321-2810 (Online), ISSN: 2321-8525 (Print)

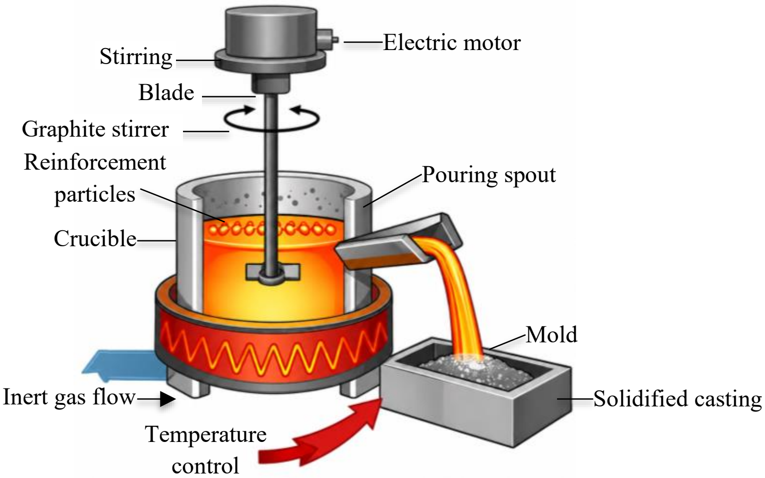

Figure 1. Schematic diagram -stir casting.

Figure 2. Adding zinc to the crucible.

Figure 3. Fap powder.

Figure 4. Molten material poured into the mould.

Figure 5. Casted rods.

The temperature of the zinc-Fap melt is closely monitored and maintained within a range of 420°C to 450°C. Maintaining this temperature ensures optimal fluidity for proper mixing and prevents premature solidification of the composite during processing. The zinc-Fap mixture is poured into a preheated mould to shape the composite. The material is allowed to solidify within the mould. Once solidified, the casting is removed and carefully inspected for any defects, ensuring the integrity of the composite, which is shown in Figure 4. After curing for 8 hours, we can get the cast rods, which are shown in Figure 5.

After casting, place the material to be annealed in the furnace, then set the furnace to 250°C. Once the temperature is reached, hold the temperature at 250°C for 3 hours. Monitor the temperature to ensure it remains within the specified range. After the 3-hour annealing period, turn off the furnace, then allow the material to cool slowly in the furnace at room temperature. Alternatively, the material can be removed and cooled in air or using a controlled cooling method, depending on the material's requirements. Machining has been done in a CNC machine with the casted samples to prepare the specimen (dumbbell-shaped), which is shown in Figure 6, and the tested samples are shown in Figure 7.

Journal of Polymer & Composites
Volume 14, Special Issue 2
ISSN: 2321-2810 (Online), ISSN: 2321-8525 (Print)

Figure 6. Specimen for tensile test.

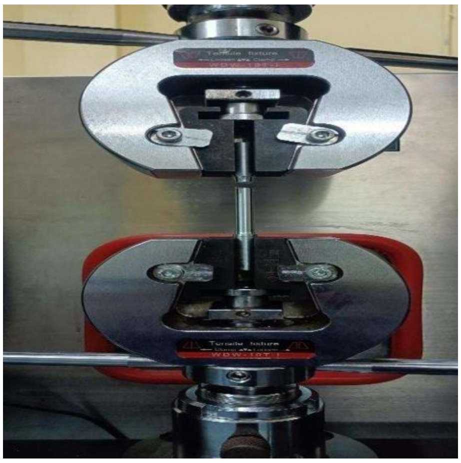

Figure 7. Sample testing in UTM.

A tensile test was conducted on samples having 1% following the ASTM A370 standard at room temperature. The specimen was of circular cross-section, with a diameter of 6.2 mm, resulting in a calculated cross-sectional area of 30.19 mm². The test was performed using a gauge length of 20 mm, which is appropriate for small-scale tensile evaluation of metallic materials.

RESULTS AND DISCUSSIONS

Optical Microscope

Figure s 8 and 9 present micrographs of the composites in their as-cast state and after etching. Both of these phenomena can be observed in the composites. The micrograph illustrates the optimal packing of the matrix, showcasing the uniform distribution of small Fap particles throughout the material.

Figure s 10–11 highlight the Etched Micrograph of Zinc reinforced with 1wt% and 2wt% Fluorapatite composites. From the above image, it is clear that when the nano fluorapatite reinforcement reached 2 wt%, the particles began to agglomerate.

Scanning Electron Microscopy (SEM)

The behavior of reinforcing particles in Zn-Fap composites was examined using scanning electron microscopy (SEM), with key findings highlighted in Figure s 12–13. As the number of nano particulates in the composite increased, SEM data revealed a greater tendency for the strengthening particles to cluster or pile up in specific regions.

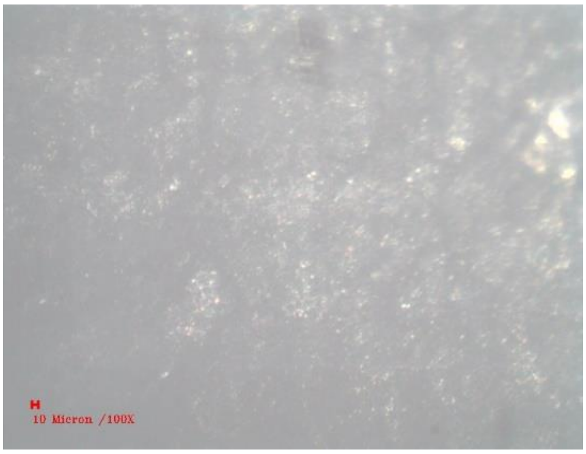

Figure 8. As -cast micrograph of Zn+1% Fap.

Figure 9. As -cast micrograph of Zn+2% Fap.

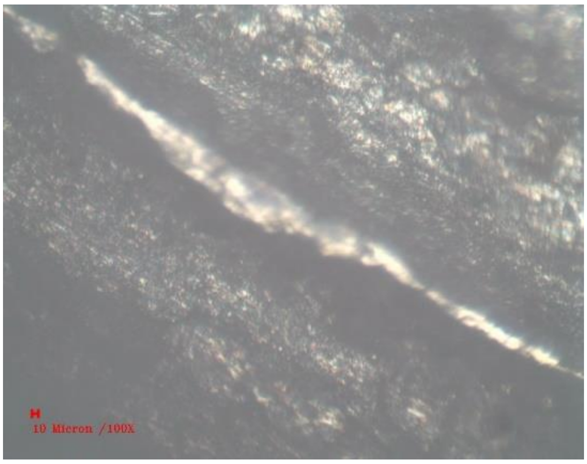

Figure 10. Etched Micrograph of Zn+1% Fap.

Figure 11. Etched Micrograph of Zn+2% Fap.

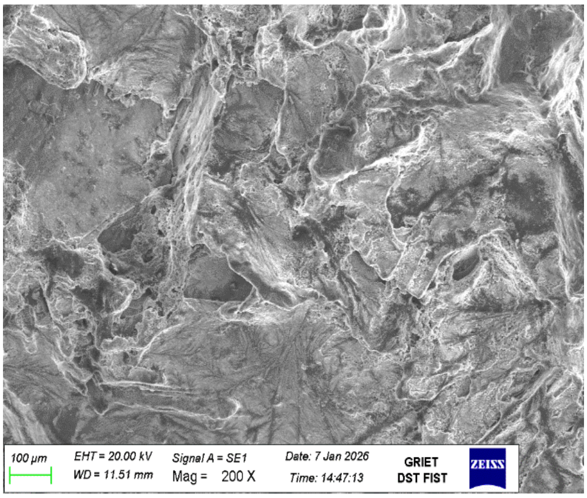

Figure 12. SEM image of Zn+1% fap.

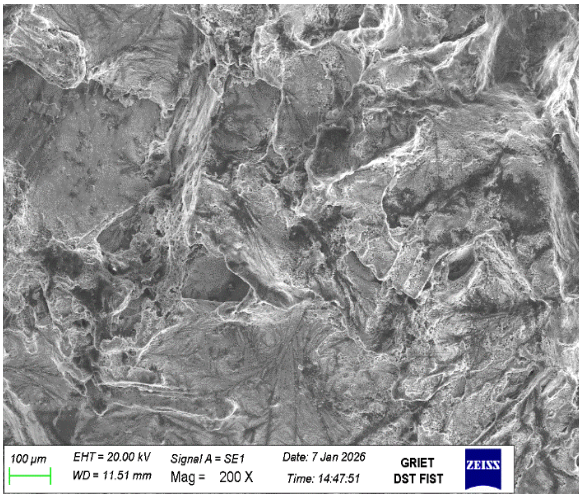

Figure 13. SEM image of Zn+2% fap.

Stress versus strain for 1% Fap specimen

The tensile test type was selected to evaluate the material's mechanical properties, including yield strength, ultimate tensile strength, and elongation, under uniaxial loading. These parameters help assess the material's compliance with mechanical performance standards and its suitability for structural or Manufacturing applications under tensile loading. The data shown in Table 1 and the concerned parameters are shown in Table 2.

Journal of Polymer & Composites
Volume 14, Special Issue 2
ISSN: 2321-2810 (Online), ISSN: 2321-8525 (Print)

Table 1. Stress versus strain of 1% fap.

S N.	Strain (%)	Sample 1 (MPa)	Sample 2 (MPa)	Sample 3 (MPa)	Average stress (MPa)
1	0	0	0	0	0
2	0.2	5.82	5.9	5.7	5.81
3	0.4	8	8.1	7.9	8
4	0.8	15	14.8	15.2	15
5	1.2	28	27.5	28.2	27.9
6	1.6	48	47.8	48.5	48.1
7	1.9	59.5	59	60	59.5
8	2	50	50.5	49.8	50.1
9	2.4	30	30.2	29.8	30
10	2.8	20	19.8	20.2	20
11	3.2	10	10.2	9.8	10
12	3.6	1	1.1	0.9	1

Table 2. Parameters for 1% fap.

S N.	Parameter	Value
1	Change in Length	20.57 mm
2	Maximum Tensile Force	1.81 kN
3	Young's Modulus (E)	2.14 GPa
4	Percentage of Elongation	3 %
5	Ultimate Tensile Stress (UTS)	60 MPa
6	Maximum Yield Stress	40 MPa
7	0.2% Offset Yield Stress	40.8 MPa

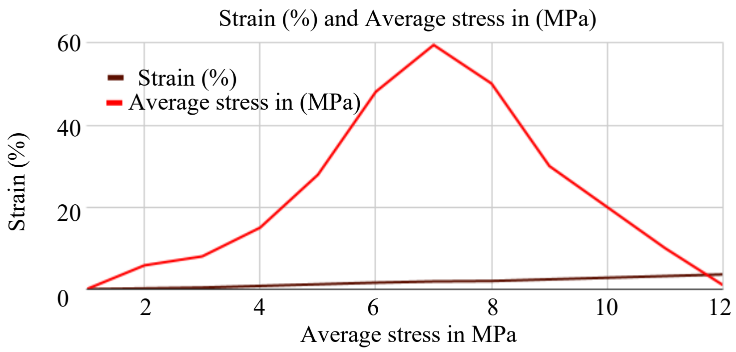

Figure 14. Stress versus strain curve of 1% fap specimen.

Based on the stress-strain curve of the 1% Fap specimen and Figure 14, the composite material exhibited an ultimate tensile stress of 60 MPa, indicating strong mechanical integrity. This peak stress reflects the effectiveness of Fap reinforcement within the zinc matrix during loading. The maximum tensile force recorded was 1.81 kN, showing the composite's ability to withstand significant axial loads before Failure. This strength supports its potential application in biomedical and lightweight engineering fields. The yield strength was calculated to be 40 MPa, while the 0.2% offset yield stress was slightly higher at 40.8 MPa, indicating a narrow elastic-to-plastic transition region.

Young's Modulus was evaluated as 2.14 GPa, which indicates moderate stiffness. This value reflects the composite's resistance to elastic deformation under stress and aligns with its use in load-bearing applications. The composite showed a 3% elongation before Failure, suggesting limited ductility. This moderate elongation ensures dimensional stability in service while providing some flexibility against mechanical stress. The change in length during testing was measured at 20.57 mm, highlighting the extent of deformation the specimen endured. This parameter assesses the composite's ability to withstand strain before fracture. Stress–strain curves from three samples exhibited consistent behavior, with all reaching maximum stress near 1.9% strain, followed by sharp drops, confirming brittle fracture characteristics after ultimate strength.

Stress versus Strain Zinc Specimen

A tensile test was performed on samples with 1% zinc content, per ASTM A370, to evaluate the material's mechanical behavior. The test was conducted at room temperature using a circular sample with a diameter of 10 mm, resulting in a cross-sectional area of 78.54 mm². The gauge length for the test was 50 mm, which is suitable for accurately capturing elongation and ductility characteristics under tensile loading. The tensile test type was selected to assess properties such as yield strength, ultimate tensile strength, and elongation, critical for material selection and quality control. The data shown in Table 3 and their corresponding parameters are shown in Table 4.

The pure zinc specimen stress-strain curve is shown in Figure 15. The tensile test was performed on pure zinc, ASTM A370, at room temperature, with a cross-sectional area of 78.54 mm² and 50 mm gauge length. The sample exhibited a maximum tensile force of 5.58 kN, corresponding to an ultimate tensile stress of 70 MPa, as indicated by the peak on the stress-strain curve. The initial elastic region indicates a Young's Modulus of 2.55 GPa, derived from the slope of the linear portion of the stress-strain curve The sample yielded at 55 MPa, and the 0.2% offset yield stress was found to be 56.1 MPa, indicating mild strain hardening behavior post-yield. The curve shows typical ductile material characteristics with a gradual increase in stress after yield until fracture occurred near 4.5% strain.

Table 3. Zinc specimen stain versus stress.

S No	Strain (%)	Stress (MPa) Sample 1	Stress (MPa) Sample 2	Stress (MPa) Sample 3	Average Stress (MPa)
1	0	0	0	0	0
2	0.25	6	6.2	5.8	6
3	0.5	8	8.1	7.9	8
4	1	9	9.3	8.7	9
5	1.5	12	12.5	11.8	12.1
6	2	24	24.2	23.8	24
7	2.5	36	36.5	35.7	36.07
8	3	48	47.8	48.3	48.03
9	3.5	58	58.2	57.7	58
10	4	66	66.3	65.8	66.03
11	4.5	72	71.5	72.3	71.93
12	4.6	2	1.8	2.2	2

Table 4. Parameters for 1% fap.

S.N.	Parameter	Value
1	Change in Length	52.6 mm
2	Maximum Tensile Force	5.58 kN
3	Young's Modulus, E	2.55 GPa
4	Percentage of Elongation	5 %
5	Ultimate Tensile Stress	70 MPa
6	Maximum Yield Stress	55 MPa
7	0.2% Offset Yield Stress	56.1 MPa

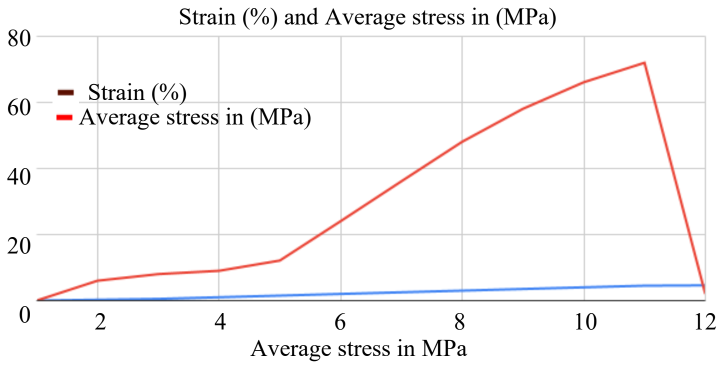

Figure 15. Stress - strain curve of zinc specimen.

The total elongation was 52.6 mm, corresponding to 5% strain, indicating moderate ductility of the tested material. A notable drop in stress after the ultimate point confirms necking and fracture, which are typical of tensile failure in ductile metals. The percentage reduction in cross-sectional area was not recorded, but visible necking suggests significant plastic deformation before fracture.

CONCLUSIONS

The comparative analysis of the tensile behavior of the 1% Fap-reinforced zinc composite and pure zinc matrix reveals significant insights into the mechanical performance and potential applications of the developed materials.

1. The 1% Fap composite demonstrated an ultimate tensile stress of 60 MPa and a yield strength of 40 MPa, with a corresponding Young's Modulus of 2.14 GPa and 3% elongation. These results confirm enhanced strength and stiffness from the reinforcement, albeit at the expense of reduced ductility, highlighting its suitability for applications requiring dimensional stability and moderate load-bearing capacity, such as biomedical implants and lightweight structural components.
2. In contrast, the pure zinc specimen exhibited higher tensile strength (70 MPa) and yield strength (55 MPa), alongside greater ductility (5% strain) and a higher Young's Modulus (2.55 GPa), indicating superior plastic deformation capabilities.
3. The stress–strain curve of the zinc sample revealed ductile Failure with pronounced necking, whereas the Fap composite showed brittle fracture behavior with abrupt Failure post-ultimate stress.

Although ductility was sacrificed, overall mechanical stability and controlled deformation properties were enhanced by adding Fap particles to the zinc matrix. These findings highlight the potential of zinc composites reinforced with Fap in specific applications where a desirable combination of strength, stiffness, and mild ductility is essential.

REFERENCES

1. Ma Y, Yang S, Meng X, et al. Heat treatment effects on microstructure and mechanical properties of CVI SiCf/PyC/SiC composites with Cansas-III SiC fibers. J Eur Ceram Soc. 2023;43(14):5940–9.
2. Lim SS, Jung SJ, Kim BK, et al. Combined hot extrusion and spark plasma sintering method for producing highly textured thermoelectric Bi2Te3 alloys. J Eur Ceram Soc. 20;40(8):3042–8.
3. Ma G, Zhu S, Wang D, et al. Effect of heat treatment on the microstructure, mechanical properties and fracture behaviors of ultra-high-strength SiC/Al–Zn–Mg–Cu composites. Int J Miner Metall Mater. 2024;31(10):2233–43.
4. Sharma A, Srinivasan K V S, Dixit M, et al. Ballistic performance of functionally graded boron carbide reinforced Al - Zn - Mg - Cu alloy. J Mater Res Technol. 2022;18:4042–59.
5. Wang Y, Zuo X, Ran S, et al. Effects of semi-solid extrusion and heat treatment on the microstructure, mechanics, and wear resistance of SiC/High aluminum zinc-base alloy composites. Mod Phys Lett B. 2020;34(25):1–14.

6. Li J, He Y, Zhao X, et al. Evolution of Microstructure and Mechanical Properties of Al-Zn-Mg-Cu Alloy by Extrusion and Heat Treatment. Coatings. 2022;12(6).
7. Huang W, Shu C, Hua L, et al. Modified bacterial outer membrane vesicles induce autoantibodies for tumor therapy. Acta Biomater. 2020;108(xxxx):300–12.
8. Murchio S, Dallago M, Zanini F, et al. Additively manufactured Ti–6Al–4V thin struts via laser powder bed fusion: Effect of building orientation on geometrical accuracy and mechanical properties. J Mech Behav Biomed Mater. 2021;119(November 2020):104495.
9. Li C, Wang X, Li B, et al. Effect of cold rolling and aging treatment on the microstructure and properties of Cu–3Ti–2Mg alloy. J Alloys Compd. 2020;818
10. Guo F, Zhou Y, Jiang Q, Chen P, Ren B. Influence of Heat Treatment Temperature on Microstructure and Mechanical Properties of TiB2@Ti/AlCoCrFeNi2.1 Eutectic High-Entropy Alloy Matrix Composites. Metals (Basel). 2025;15(7):1–14.
11. Zhou J, Ye F, Cheng L, Li M, Cui X, Fu Z, et al. Effects of heat treatment on mechanical properties of 3D Si3N4f/BN/Si3N4 composites by PIP. J Eur Ceram Soc. 2021;41(14):6905–14.
12. Chung PP, EsFahani M, Wang J, et al. Effects of heat treatment on microstructure evolution and corrosion performance of mechanically plated zinc coatings. Surf Coatings Technol. 2019;377(August):124916.
13. Xu M, Teng X, Yang C, et al. Effect of heat treatment on microstructure and mechanical properties of Mg94Zn2Y4 alloy. Xiyou Jinshu Cailiao Yu Gongcheng/Rare Met Mater Eng. 2016;45(11):2804–8.
14. Khabiri G, Aboraia AM, Soliman M, et al. A novel α-Fe2O3@MoS2QDs heterostructure for enhanced visible-light photocatalytic performance using ultrasonication approach. Ceram Int. 2020;46(11):19600–8.
15. Lee H, Song MY, Ryu S, et al. Acetaldehyde oxidation under high humidity using a catalytic non-thermal plasma system over Mn-loaded Y zeolites. Mater Lett. 2020;262(xxxx):127051.
16. Wu J, Xu X, Zhang X, et al. Effect of Heat Treatment on Microstructure and Mechanical Properties of Multiscale SiCp Hybrid Reinforced 6061 Aluminum Matrix Composites. J Wuhan Univ Technol Sci Ed. 2024;39(1):174–81.
17. Xie Y, Zeng G, Zhang Y, et al. Time lapsed corrosion behavior of Zn-Mg composites fabricated by low-temperature sintering in simulated body fluid. Compos Commun. 2025;57:102445.
18. Li M, Zhu Z, Zhang L, et al. Enhancement of mechanical, corrosion, and biocompatibility properties of zinc alloys through magnesium and neodymium alloying for bone implant applications. RSC Adv. 2025;15(53):45438–52.
19. Vencl A, Šljivić V, Pokusová M, et al. Production, Microstructure and Tribological Properties of Zn-Al/Ti Metal-Metal Composites Reinforced with Alumina Nanoparticles. Int J Met. 2021;15(4):1402–11.
20. Dai Q, Peng S, Zhang Z, et al. Microstructure and Mechanical Properties of Zinc Matrix Biodegradable Composites Reinforced by Graphene. 2021;9(March):1–14.
21. Jiang P, Yang Y, Xie S, et al. Highly efficient and selective removal of U(VI) from acidic aqueous solution by chitosan/fluorapatite composite. J Radioanal Nucl Chem [Internet]. 2024;333(8):3921–35. Available from: http://dx.doi.org/10.1007/s10967-024-09553-z

